

Three-Phase Equilibrium Relations and Hydrate Dissociation Enthalpies for Hydrofluorocarbon Hydrate Systems: HFC-134a, -125, and -143a Hydrates

Shunsuke Hashimoto,^{*,‡} Takashi Makino,[†] Yoshiro Inoue,[‡] and Kazunari Ohgaki[‡]

Division of Chemical Engineering, Department of Materials Engineering Science, Graduate School of Engineering Science, Osaka University, 1-3 Machikaneyama, Toyonaka, Osaka 560-8531, Japan, and Research Center for Compact Chemical System, National Institute of Advanced Industrial Science and Technology (AIST), 4-2-1 Nigatake, Miyagino-ku, Sendai 983-8551, Japan

The three-phase equilibrium (pressure–temperature) relations were measured for the hydrofluorocarbon (HFC) (1,1,1,2-tetrafluoroethane (-134a), pentafluoroethane (-125), or 1,1,1-trifluoroethane (-143a)) + water binary systems containing gas hydrate. The measurements were performed in the pressure range up to 10.0 MPa and the temperature range of (273.15 to 295.15) K. The invariant quadruple points (gaseous HFC, liquid HFC, aqueous, and hydrate phases) were located at 283.19 K and 0.416 MPa (HFC-134a), 283.95 K and 0.930 MPa (HFC-125), and 283.33 K and 0.838 MPa (HFC-143a), respectively. The enthalpies of hydrate dissociation to gaseous HFC and water were calculated with the Clapeyron equation, and the value was about 140 kJ·mol⁻¹ for all HFC hydrate systems.

Introduction

Gas hydrate is a clathrate inclusion compound. It consists of host water molecules and appropriate relatively small guest molecules. The water molecules are hydrogen-bonded and constitute the hydrate frameworks with cavities, in which guest molecules are encaged. In general, the van der Waals interaction (attractive and repulsive forces) operates on the guest and water molecules, and the guest molecules encaged in the clathrate hydrate do not join in hydrogen bonds of water molecules.¹ There are several types of hydrate unit-cells, and in particular, two types, which are called structure-I (s-I) and structure-II (s-II), are well-known. Both the hydrate unit cells include the pentagonal dodecahedron (5¹², S-cage). In addition to the S-cage, the s-I and s-II hydrates have the tetrakaidecahedron (5¹²6², M-cage) and the hexakaidecahedron (5¹²6⁴, L-cage), respectively. The unit cell of s-I is composed of two S-cages and six M-cages, while that of s-II consists of 16 S-cages and 8 L-cages. The hydrate structure mainly depends on temperature, pressure, and the physical and chemical properties of guest species.

Some of the unique properties of gas hydrate are the large dissociation enthalpy and proper melting temperature for refrigerating and air-conditioning. Therefore, the gas hydrate has attracted considerable attention as a promising phase change material (PCM) for the refrigerating and air-conditioning systems. Especially in the case of the gas hydrate being stable at relatively low pressures and (278 to 284) K (the temperature range of the chilled water),² the gas hydrate thermal storage system can work with higher coefficient of performance than the ice thermal storage system.³ Consequently, it is possible to save about 40 % energy by the use of gas hydrate as a refrigerant.^{2,3}

The equilibrium pressures of some hydrofluorocarbon (HFC) hydrates are relatively lower (less than 1 MPa) than those of conventional hydrocarbon gas hydrates. On the other hand, the

dissociation enthalpies of the HFC hydrate are comparable with those of ordinary hydrocarbon gas hydrates. Some HFCs have been used as alternative refrigerants for the air-conditioning system to replace chlorofluorocarbons (CFCs) and chlorohydrofluorocarbons (CHFCs), which have high ozone depletion and global warming potentials.⁴ The HFC has specific thermal and chemical characteristics that are favorable as a refrigerant material. However, the reduction of HFC use is required by Kyoto Protocol because of its relatively high global-warming potential. In our recent study,⁵ based on the phase-equilibrium relation, we have estimated that the dissociation enthalpy of difluoromethane (HFC-32) hydrate (gas hydrate to gaseous HFC and water) is about 70 kJ·mol⁻¹ near the freezing point. The dissociation enthalpy per mole of gas of the HFC-32 hydrate is higher than the vaporization enthalpy per mole of gas of HFC-32. Therefore, the employment of the slurry containing gas hydrate is considered as an effective technique to decrease the amount of HFC in the cool energy storage system.

Phase change data and hydrate dissociation enthalpies, especially for simple HFC hydrate systems, are surely essential to develop the air-conditioning and refrigerating processes with HFC hydrates. Some previous studies^{6–10} reported the equilibrium (pressure–temperature) relations and dissociation enthalpies of the halogenated–hydrocarbon hydrate systems. However, the number of investigated systems is very limited, and an appropriate HFC hydrate system for the cool energy storage system is still unclear. Therefore, further fundamental studies such as phase equilibrium measurement for HFC hydrates should be performed.

In the present study, three-phase equilibrium (pressure–temperature) relations for three binary systems (1,1,1,2-tetrafluoroethane (HFC-134a), pentafluoroethane (HFC-125), or 1,1,1-trifluoroethane (HFC-143a) + water systems) have been investigated accurately by phase-equilibrium measurement. In addition, the hydrate dissociation enthalpies (gas hydrate to gaseous HFC and water) have been calculated with the Clapeyron equation.

* Corresponding author. Telephone & Fax: +81-6-6850-6277. E-mail: shunsuke@cheng.es.osaka-u.ac.jp.

[†] National Institute of Advanced Industrial Science and Technology (AIST).

[‡] Osaka University.

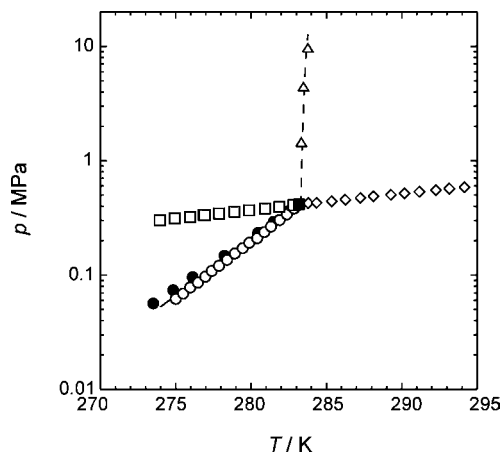


Figure 1. Three-phase equilibrium relation (temperature T –pressure p projection) for the HFC-134a (2) + water (1) binary system. ●, HL₁G (Liang et al., 2001); ○, HL₁G (present study); □, HL₂G (present study); △, HL₁L₂ (present study); ◇, L₁L₂G (present study); ■, quadruple point (Q₂, present study); –, the reference data (Akiya et al., 1999).

Experimental Methods

Experimental Apparatus. The experimental equipment including a high-pressure glass cell was the same as a previous one.⁵ The inner volume and maximum working pressure of the high-pressure glass cell were 10 cm³ and 5 MPa, respectively.

The temperature was measured within an uncertainty of 0.02 K using a thermistor probe (model: Takara D-632). The probe was calibrated with a Pt resistance thermometer (25 Ω) defined by ITS-90. The pressure was measured by a pressure gauge (model: Valcom VPRT) calibrated by a RUSKA quartz Bourdon tube gauge (model: direct reading pressure gauge, series 6000). The estimated uncertainty of equilibrium pressure was 0.001 MPa ($p < 1$ MPa) or 0.01 MPa ($p > 1$ MPa).

Experimental Procedure. Almost all procedures of phase equilibrium measurements in the present study were the same as a previous one.⁵ In advance, the dissolved air in water was sufficiently degassed and replaced by a bubbling method with each HFC gas. After that, the degassed water was introduced into the evacuated high-pressure glass cell. The cell was immersed in a thermo-controlled water bath to control the temperature. Then, the contents were pressurized by supplying HFC gas up to a desired pressure and subcooled and agitated to generate the gas hydrate. A magnetic stirrer was manipulated in a vertical direction to agitate the contents. The phase behavior was observed directly under the transmitted light. After the formation of gas hydrate, the pressure dropped and reached a plateau, which meant the three-phase equilibrium state of hydrate (H), gas (G), and water (L₁) was established. Then, the pressure and temperature were determined as the three-phase equilibrium pressure and temperature, respectively. In the present study, in addition to the three-phase equilibrium curve of HL₁G, other curves of HL₂G and L₁L₂G were also measured by means of similar procedures. The symbol L₂ stands for the liquid HFC phase.

Unlike the equilibrium measurement for HL₁G, HL₂G, and L₁L₂G conditions, the three-phase equilibrium curve of HL₁L₂ was measured with another high-pressure cell (maximum working pressure was 100 MPa).⁵ A certain amount of gaseous HFC was introduced into the evacuated high-pressure optical cell, and then the distilled water was charged up to a desired pressure by use of the high-pressure pump. After the pressurization, the two-phase coexistence state of HFC hydrate + water appeared immediately under the experimental conditions. There-

Table 1. Three-Phase Equilibrium Data (Temperature T , Pressure p) of the HFC-134a (2) + Water (1) Binary System

| T /K | | p /MPa |
|--------|---|----------|
| | HL ₁ G | |
| 275.00 | | 0.062 |
| 275.48 | | 0.069 |
| 275.96 | | 0.078 |
| 276.47 | | 0.086 |
| 276.96 | | 0.097 |
| 277.39 | | 0.109 |
| 277.87 | | 0.121 |
| 278.40 | | 0.136 |
| 278.92 | | 0.155 |
| 279.45 | | 0.172 |
| 279.88 | | 0.192 |
| 280.41 | | 0.210 |
| 280.88 | | 0.238 |
| 281.32 | | 0.266 |
| 281.89 | | 0.304 |
| 282.38 | | 0.341 |
| 282.86 | | 0.383 |
| 283.17 | | 0.412 |
| | HL ₂ G | |
| 273.95 | | 0.302 |
| 274.94 | | 0.313 |
| 275.95 | | 0.323 |
| 276.86 | | 0.335 |
| 276.93 | | 0.335 |
| 277.88 | | 0.346 |
| 278.90 | | 0.358 |
| 279.87 | | 0.370 |
| 280.92 | | 0.382 |
| 281.88 | | 0.395 |
| 282.81 | | 0.410 |
| | L ₁ L ₂ G | |
| 283.81 | | 0.424 |
| 284.36 | | 0.427 |
| 285.37 | | 0.441 |
| 286.27 | | 0.455 |
| 287.28 | | 0.471 |
| 288.15 | | 0.486 |
| 289.30 | | 0.502 |
| 290.20 | | 0.518 |
| 291.19 | | 0.534 |
| 292.28 | | 0.552 |
| 293.18 | | 0.569 |
| 294.19 | | 0.586 |
| | HL ₁ L ₂ | |
| 283.34 | | 1.45 |
| 283.49 | | 4.42 |
| 283.78 | | 9.68 |
| | Q ₂ (HL ₁ L ₂ G) | |
| 283.19 | | 0.416 |

after, the temperature was increased gradually to generate the liquid HFC phase by dissociation of the gas hydrate. The gas hydrate was annealed by giving temperature perturbations to avoid a hysteresis effect. The contents were agitated intermittently for at least half a day. After the pressure change per hour was within 0.01 MPa, the pressure and temperature were determined as the three-phase equilibrium pressure and temperature, respectively.

In the present study, to confirm the experimental reproducibility without a hysteresis phenomenon, we repeated each equilibrium measurement using fresh water.

Materials. HFC-134a (mole fraction purity, > 99.6 %) and HFC-125 (mole fraction purity, > 99.5 %) were purchased from Daikin Industries, Ltd. HFC-143a (mole fraction purity, > 99.5 %) was obtained from Du pont-Mitsui Fluorochemicals Co., Ltd. The critical temperature and pressure of HFC-134a, HFC-125, and HFC-143a were (374.21 K and 4.06 MPa), (339.17 K

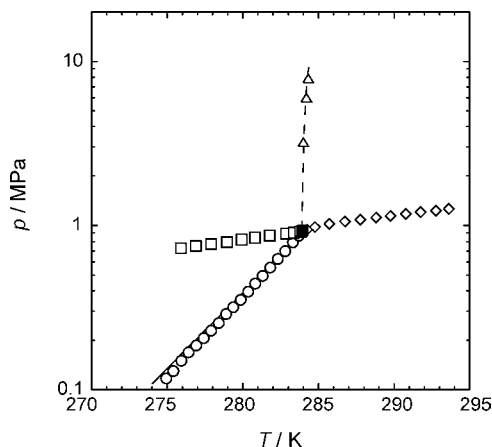


Figure 2. Three-phase equilibrium relation (temperature T –pressure p projection) for the HFC-125 (2) + water (1) binary system. \circ , HL₁G (present study); \square , HL₂G (present study); \triangle , HL₁L₂ (present study); \diamond , L₁L₂G (present study); \blacksquare , quadruple point (Q_2 , present study). $-$, the reference data (Akiya et al., 1999).

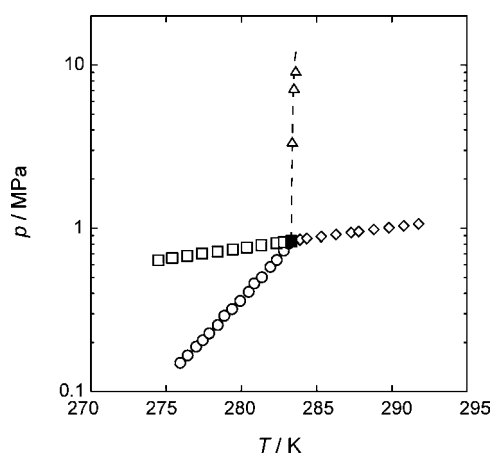


Figure 3. Three-phase equilibrium relation (temperature T –pressure p projection) for the HFC-143a (2) + water (1) binary system. \circ , HL₁G (present study); \square , HL₂G (present study); \triangle , HL₁L₂ (present study); \diamond , L₁L₂G (present study); \blacksquare , quadruple point (Q_2 , present study).

and 3.62 MPa), and (345.86 K and 3.76 MPa), respectively.¹¹ Distilled water was obtained from Wako Pure Chemical Industries, Ltd. All the materials were used without further purification.

Results and Discussion

Figure 1 shows the three-phase equilibria for the HFC-134a + water binary system. Table 1 summarizes the three-phase equilibrium (pressure (p)–temperature (T)) relations of HL₁G, HL₂G, HL₁L₂, and L₁L₂G. A filled square is located at the invariant quadruple point (Q_2) of HL₁L₂G. As shown in Figure 1, the HL₁G curve agrees well with the reported equilibrium relations.^{7,8} Four three-phase equilibrium curves converge at the Q_2 , and the quadruple point is determined as (283.19 K and 0.416 MPa).

The three-phase equilibrium (p – T) relations of HL₁G, HL₂G, HL₁L₂, and L₁L₂G for the HFC-125 or -143a + water binary systems are also shown in Figures 2 and 3 and summarized in Tables 2 and 3, respectively. The phase behaviors of the HFC-125 and HFC-143a hydrate systems are similar to that of the simple HFC-134a hydrate system. The quadruple points for the HFC-125 + water and HFC-143a + water systems are located at (283.95 K and 0.930 MPa) and (283.33 K and 0.838 MPa),

Table 2. Three-Phase Equilibrium Data (Temperature T , Pressure p) of the HFC-125a (2) + Water (1) Binary System Containing Gas Hydrates

| T/K | | p/MPa |
|--------|--|---------|
| | HL ₁ G | |
| 274.94 | | 0.117 |
| 275.40 | | 0.130 |
| 275.94 | | 0.150 |
| 276.41 | | 0.169 |
| 276.92 | | 0.186 |
| 277.41 | | 0.206 |
| 277.91 | | 0.229 |
| 278.41 | | 0.255 |
| 278.90 | | 0.289 |
| 279.37 | | 0.318 |
| 279.86 | | 0.353 |
| 280.35 | | 0.396 |
| 280.82 | | 0.444 |
| 281.31 | | 0.495 |
| 281.81 | | 0.556 |
| 282.31 | | 0.628 |
| 282.80 | | 0.701 |
| 283.31 | | 0.792 |
| 283.70 | | 0.870 |
| | HL ₂ G | |
| 275.90 | | 0.730 |
| 276.89 | | 0.752 |
| 277.90 | | 0.772 |
| 278.94 | | 0.794 |
| 279.93 | | 0.820 |
| 280.81 | | 0.843 |
| 281.79 | | 0.867 |
| 282.86 | | 0.892 |
| 283.37 | | 0.904 |
| 283.79 | | 0.918 |
| | L ₁ L ₂ G | |
| 284.27 | | 0.941 |
| 284.78 | | 0.976 |
| 285.73 | | 1.02 |
| 286.76 | | 1.05 |
| 287.78 | | 1.08 |
| 288.81 | | 1.11 |
| 289.77 | | 1.14 |
| 290.78 | | 1.17 |
| 291.76 | | 1.20 |
| 292.78 | | 1.23 |
| 293.63 | | 1.26 |
| | HL ₁ L ₂ | |
| 284.01 | | 3.21 |
| 284.21 | | 6.00 |
| 284.34 | | 7.87 |
| | Q_2 (HL ₁ L ₂ G) | |
| 283.95 | | 0.930 |

respectively. Additionally, as shown in Figure 4, the isothermal equilibrium pressure of the HFC-125 hydrate is almost the same as that of the HFC-143a hydrate under HL₁G conditions, while the HFC-134a hydrate is stable under lower pressures than the HFC-125 and HFC-143a hydrates. The HFC-134a hydrate slurry has a larger prospect as a refrigerant for air-conditioning than the other systems measured in the present study. In addition, all the present hydrate systems have similar gradients of HL₁G curves.

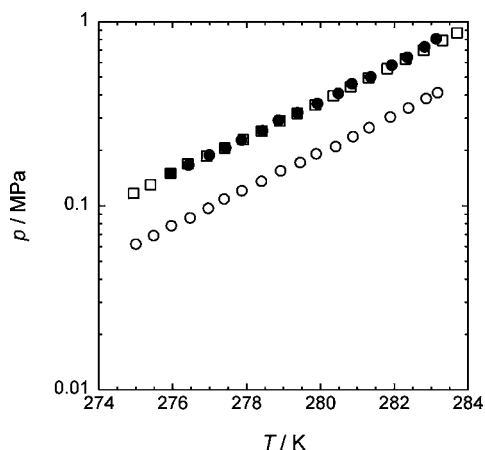
The slope of the three-phase equilibrium curve ($(dp/dT)_{eq}$) was calculated at each equilibrium data point on the HL₁G curve. From the combination of $(dp/dT)_{eq}$, molar volumes of HFC hydrate (v^H), water ($v^L_{H_2O}$), and gaseous HFC (v^G_{HFC}), the hydrate dissociation enthalpy per unit hydrate ($\Delta_{hyd}H$) was calculated with the Clapeyron equation as follows

$$(dp/dT)_{eq} = \Delta_{hyd}H/(\Delta_{hyd}VT) \quad (1)$$

Table 3. Three-Phase Equilibrium Data (Temperature T , Pressure p) of the HFC-143a (2) + Water (1) Binary System Containing Gas Hydrates

| T/K | p/MPa |
|---|---------|
| HL ₁ G | |
| 275.94 | 0.150 |
| 276.43 | 0.167 |
| 276.99 | 0.189 |
| 277.43 | 0.207 |
| 277.86 | 0.228 |
| 278.43 | 0.256 |
| 278.86 | 0.292 |
| 279.38 | 0.321 |
| 279.92 | 0.360 |
| 280.48 | 0.409 |
| 280.85 | 0.461 |
| 281.36 | 0.503 |
| 281.93 | 0.582 |
| 282.35 | 0.642 |
| 282.82 | 0.732 |
| 283.13 | 0.810 |
| HL ₂ G | |
| 274.49 | 0.640 |
| 275.41 | 0.660 |
| 276.40 | 0.680 |
| 277.39 | 0.702 |
| 278.42 | 0.723 |
| 279.42 | 0.745 |
| 280.36 | 0.766 |
| 281.32 | 0.789 |
| 282.33 | 0.811 |
| 282.84 | 0.824 |
| 283.32 | 0.836 |
| L ₁ L ₂ G | |
| 283.90 | 0.849 |
| 283.91 | 0.851 |
| 284.36 | 0.863 |
| 285.31 | 0.887 |
| 286.30 | 0.912 |
| 287.31 | 0.938 |
| 287.80 | 0.952 |
| 288.82 | 0.978 |
| 289.82 | 1.01 |
| 290.80 | 1.03 |
| 291.79 | 1.06 |
| HL ₁ L ₂ | |
| 283.39 | 3.37 |
| 283.51 | 7.21 |
| 283.62 | 9.20 |
| Q ₂ (HL ₁ L ₂ G) | |
| 283.33 | 0.838 |

where the total molar volume change for hydrate formation or dissociation, $\Delta_{\text{hyd}}V$, is defined by eq 2

**Figure 4.** Three-phase (HL₁G) equilibrium curves of HFC-134a, -125, and -143a + water systems. ○, HFC-134a; □, HFC-125; ●, HFC-143a.

$$\Delta_{\text{hyd}}V = v_{\text{HFC}}^{\text{G}} + qv_{\text{H}_2\text{O}}^{\text{L}} - v^{\text{H}} \quad (2)$$



On the basis of the molecular size of HFC obtained from reference data,⁶ all HFCs investigated in the present study are the s-II former and occupy only the L-cages of s-II. Therefore, v^{H} was $390 \text{ cm}^3 \cdot \text{mol}^{-1}$, which was calculated from the lattice constant of s-II (1.73 nm),¹² and the hydration number, q , was assumed to be 17 (ideal hydration, $\text{HFC} \cdot 17\text{H}_2\text{O}$). $v_{\text{H}_2\text{O}}^{\text{L}}$ was calculated from the equation proposed by Saul and Wagner.¹³ In addition, $v_{\text{HFC}}^{\text{G}}$ was obtained from the Lee–Kesler equation of state¹⁴ (for details, refer to Supporting Information).

Table 4. Hydrate Dissociation Enthalpy (Gas Hydrate to Gaseous HFC and Water), $\Delta_{\text{hyd}}H$, of the Three HFC (HFC-134a, -125, and -143a) Hydrates

| T K | $v_{\text{HFC}}^{\text{G}}$ $\text{cm}^3 \cdot \text{mol}^{-1}$ | $v_{\text{H}_2\text{O}}^{\text{L}}$ $\text{cm}^3 \cdot \text{mol}^{-1}$ | $\Delta_{\text{hyd}}V$ $\text{cm}^3 \cdot \text{mol}^{-1}$ | $(dp/dT)_{\text{eq}}$ $\text{MPa} \cdot \text{K}^{-1}$ | $\Delta_{\text{hyd}}H$ $\text{kJ} \cdot \text{mol}^{-1}$ |
|----------|--|--|---|---|---|
| HFC-134a | | | | | |
| 275.00 | 36276 | 18.0175 | 36192 | 0.014 | 142.32 |
| 275.48 | 32594 | 18.0172 | 32510 | 0.016 | 143.07 |
| 275.96 | 28817 | 18.0169 | 28733 | 0.018 | 141.51 |
| 276.47 | 26131 | 18.0167 | 26048 | 0.020 | 144.57 |
| 276.96 | 23144 | 18.0176 | 23060 | 0.023 | 143.57 |
| 277.39 | 20564 | 18.0164 | 20480 | 0.025 | 141.03 |
| 277.87 | 18499 | 18.0164 | 18416 | 0.028 | 141.91 |
| 278.40 | 16427 | 18.0164 | 16343 | 0.031 | 142.60 |
| 278.92 | 14369 | 18.0164 | 14285 | 0.035 | 140.80 |
| 279.45 | 12916 | 18.0166 | 12833 | 0.040 | 143.21 |
| 279.88 | 11527 | 18.0167 | 11444 | 0.044 | 141.26 |
| 280.41 | 10510 | 18.0170 | 10426 | 0.050 | 145.72 |
| 280.88 | 9219 | 18.0172 | 9136 | 0.056 | 142.55 |
| 281.32 | 8199 | 18.0174 | 8115 | 0.061 | 140.38 |
| 281.89 | 7113 | 18.0178 | 7030 | 0.070 | 138.98 |
| 282.38 | 6286 | 18.0181 | 6203 | 0.079 | 137.55 |
| 282.86 | 5538 | 18.0185 | 5455 | 0.088 | 135.36 |
| 283.17 | 5110 | 18.0187 | 5026 | 0.094 | 134.13 |
| HFC-125 | | | | | |
| 274.94 | 19061 | 18.0171 | 18977 | 0.027 | 138.74 |
| 275.40 | 17138 | 18.0167 | 17054 | 0.030 | 138.60 |
| 275.94 | 14820 | 18.0163 | 14736 | 0.033 | 135.61 |
| 276.41 | 13124 | 18.0160 | 13040 | 0.037 | 133.71 |
| 276.92 | 11905 | 18.0168 | 11821 | 0.042 | 136.31 |
| 277.41 | 10723 | 18.0156 | 10640 | 0.047 | 137.32 |
| 277.91 | 9617 | 18.0154 | 9534 | 0.052 | 138.05 |
| 278.41 | 8605 | 18.0153 | 8521 | 0.058 | 138.44 |
| 278.90 | 7550 | 18.0153 | 7467 | 0.065 | 135.78 |
| 279.37 | 6831 | 18.0153 | 6747 | 0.073 | 136.71 |
| 279.86 | 6117 | 18.0153 | 6032 | 0.081 | 136.84 |
| 280.35 | 5411 | 18.0153 | 5327 | 0.091 | 135.22 |
| 280.82 | 4781 | 18.0154 | 4697 | 0.101 | 132.86 |
| 281.31 | 4245 | 18.0154 | 4161 | 0.113 | 131.75 |
| 281.81 | 3731 | 18.0155 | 3647 | 0.126 | 129.55 |
| 282.31 | 3250 | 18.0156 | 3166 | 0.141 | 126.17 |
| 282.80 | 2862 | 18.0157 | 2778 | 0.158 | 123.90 |
| 283.31 | 2474 | 18.0157 | 2390 | 0.177 | 119.89 |
| 283.70 | 2204 | 18.0157 | 2120 | 0.193 | 116.32 |
| HFC-143a | | | | | |
| 275.94 | 14818 | 18.0163 | 14734 | 0.034 | 138.01 |
| 276.43 | 13286 | 18.0160 | 13202 | 0.038 | 138.74 |
| 276.99 | 11709 | 18.0157 | 11625 | 0.043 | 139.33 |
| 277.43 | 10667 | 18.0155 | 10584 | 0.048 | 140.65 |
| 277.86 | 9657 | 18.0154 | 9573 | 0.053 | 140.73 |
| 278.43 | 8567 | 18.0153 | 8484 | 0.060 | 142.56 |
| 278.86 | 7464 | 18.0152 | 7380 | 0.067 | 137.18 |
| 279.38 | 6760 | 18.0152 | 6676 | 0.075 | 140.20 |
| 279.92 | 5987 | 18.0153 | 5903 | 0.085 | 140.72 |
| 280.48 | 5222 | 18.0153 | 5138 | 0.097 | 139.69 |
| 280.85 | 4583 | 18.0152 | 4499 | 0.106 | 133.40 |
| 281.36 | 4167 | 18.0154 | 4083 | 0.119 | 136.45 |
| 281.93 | 3538 | 18.0155 | 3455 | 0.136 | 131.98 |
| 282.35 | 3163 | 18.0155 | 3079 | 0.149 | 129.83 |
| 282.82 | 2711 | 18.0154 | 2628 | 0.167 | 123.70 |
| 283.13 | 2398 | 18.0152 | 2314 | 0.179 | 117.14 |

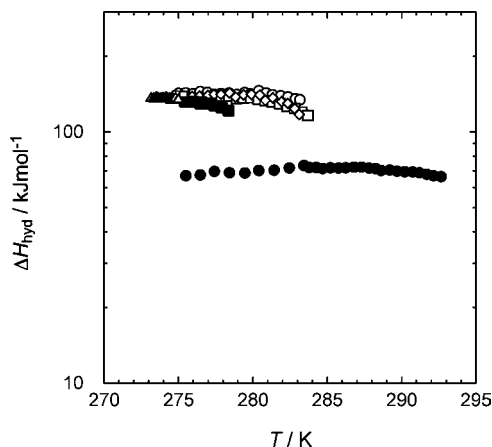


Figure 5. Temperature dependence of hydrate dissociation enthalpies (gas hydrate to gaseous HFC and water), ΔH_{hyd} , for the each HFC hydrate. ●, HFC-32 hydrate (Hashimoto et al., in press); ■, C_3H_8 hydrate (Kubota et al., 1984); △, $i\text{-C}_4\text{H}_{10}$ hydrate (Rouher and Barduhn, 1969); ○, HFC-134a hydrate; □, HFC-125 hydrate; ◇, HFC-143a hydrate.

The values of $(dp/dT)_{\text{eq}}$ were obtained from the fitting data of three-phase (HL_1G) equilibrium curve on the p – T relation. Hence, the hydrate dissociation enthalpies, ΔH_{hyd} , can be calculated and are summarized in Table 4, and the temperature dependencies of the enthalpy are shown in Figure 5. The dissociation enthalpies of the investigated HFC hydrates decrease very gradually with an increase of temperature. Each of the investigated HFC hydrates shows a similar value of dissociation enthalpy, about $140 \text{ kJ}\cdot\text{mol}^{-1}$ near the freezing point. This heat quantity is comparable with the dissociation enthalpies of the simple C_3H_8 hydrate¹⁵ and $i\text{-C}_4\text{H}_{10}$ hydrate¹⁶ and larger than that of the simple HFC-32 hydrate.⁵

Conclusion

Four three-phase equilibrium curves of HL_1G , HL_2G , HL_1L_2 , and $\text{L}_1\text{L}_2\text{G}$ (without hydrate phase) for the binary systems of HFC-134a, -125, or -143a + water have been measured in the temperature range from (273.15 to 295.15) K and pressure range up to 10.0 MPa. The HFC-134a hydrate has the lowest equilibrium pressure under the HL_1G conditions in the tested hydrate systems. The invariant quadruple points, Q_2 ($\text{HL}_1\text{L}_2\text{G}$), are determined as follows: HFC-134a system (283.19 K and 0.416 MPa), HFC-125 system (283.95 K and 0.930 MPa), and HFC-143a system (283.33 K and 0.838 MPa). The dissociation enthalpies of the present HFC hydrates (gas hydrate to gaseous HFC and water), which were calculated with the Clapeyron equation, are about $140 \text{ kJ}\cdot\text{mol}^{-1}$ near the freezing point and larger than that of the simple HFC-32 hydrate.

Acknowledgment

The authors are grateful to the Division of Chemical Engineering, Graduate School of Engineering Science, Osaka University, for the

scientific support by Gas-Hydrate Analyzing System (GHAS). The authors give their thanks to Drs. Y. Egashira, H. Sato, and T. Sugahara (Osaka University) for the valuable discussion and suggestions.

Supporting Information Available:

Details of the Lee–Kesler method. This material is available free of charge via the Internet at <http://pubs.acs.org>.

Literature Cited

- (1) Sloan, E. D., Jr.; Koh, C. A. *Clathrate Hydrates of Natural Gases*, 3rd ed.; Taylor & Francis: New York, 2008.
- (2) Hensel, E. C.; Robinson, N. L.; Buntain, J.; Glover, J. W.; Birdsell, B. D.; Sohn, C. W. Chilled-Water Thermal Storage System Performance Monitoring. *ASHRAE Trans.* **1991**, *97*, 1151–1160.
- (3) Knebel, D. E. Predicting and Evaluating the Performance of Ice Harvesting Thermal Energy Storage Systems. *ASHRAE Trans.* **1995**, *101*, 22–39.
- (4) Fialho, P. S.; Nieto de Castro, C. A. Prediction of Halocarbon Liquid Densities by a Modified Hard Sphere-De Santis Equation of State. *Fluid Phase Equilib.* **1996**, *118*, 103–114.
- (5) Hashimoto, S.; Miyauchi, H.; Inoue, Y.; Ohgaki, K. Thermodynamic and Raman Spectroscopic Studies on Difluoromethane (HFC-32) + water Binary System. *J. Chem. Eng. Data* **2010**, DOI: je9009859.
- (6) Brouwer, D. H.; Brouwer, E. B.; Maclaurin, G.; Lee, M.; Parks, D.; Ripmeester, J. A. Some New Halogen-containing Hydrate-formers for Structure I and II Clathrate Hydrates. *Supramol. Chem.* **1997**, *8*, 361–367.
- (7) Akiya, T.; Shimazaki, T.; Oowa, M.; Matsuno, M.; Yoshida, Y. Formation Conditions of Clathrates Between HFC Alternative Refrigerants and Water. *Int. J. Thermodyn.* **1999**, *20*, 1753–1763.
- (8) Liang, D.; Guo, K.; Wang, R.; Fan, S. Hydrate Equilibrium Data of 1,1,1,2-tetrafluoroethane (HFC-134a), 1,1-dichloro-1-fluoroethane (HCFC-141b) and 1,1-difluoroethane (HFC-152a). *Fluid Phase Equilib.* **2001**, *187–188*, 61–70.
- (9) Imai, S.; Okutani, K.; Ohmura, R.; Mori, Y. H. Phase Equilibrium for Clathrate Hydrates Formed with Difluoromethane + either Cyclopentane or Tetra-*n*-butylammonium Bromide. *J. Chem. Eng. Data* **2005**, *50*, 1783–1786.
- (10) Imai, S.; Miyake, K.; Ohmura, R.; Mori, Y. H. Phase Equilibrium for Clathrate Hydrates Formed with Difluoromethane or Krypton, Each Coexisting with Fluorocyclopentane. *J. Chem. Eng. Data* **2006**, *51*, 2222–2224.
- (11) Lemmon, E. W.; Huber, M. L.; McLinden, M. O. *NIST Reference Fluid Thermodynamic and Transport Properties - REFPROP ver. 8.0*, NIST Standard Reference Database 23; NIST: Gaithersburg, MD, 2007.
- (12) von Stackelberg, M. Feste Gashydrate. *Naturwissenschaften* **1949**, *36*, 327–333.
- (13) Saul, A.; Wagner, W. A Fundamental Equation for Water Covering the Range from the Melting Line to 1273 K at Pressures up to 25000 MPa. *J. Phys. Chem. Ref. Data* **1989**, *18*, 1537–1564.
- (14) Reid, R. C.; Prausnitz, J. M.; Poling, B. E. *The Properties of Gases & Liquids*, 4th ed.; McGraw-Hill Book Company: New York, 1986; pp 47–49.
- (15) Kubota, H.; Shimizu, K.; Tanaka, Y.; Makita, T. Thermodynamic Properties of R13 (Chlorotrifluoromethane), R23 (Trifluoromethane), R152a (Difluoroethane), and Propane hydrates for Desalination of Seawater. *J. Chem. Eng. Jpn.* **1984**, *17*, 423–429.
- (16) Rouher, O. S.; Barduhn, A. J. Hydrates of iso- and n-butane and their mixtures. *Desalination* **1969**, *6*, 57–73.

Received for review May 20, 2010. Accepted July 23, 2010.

JE100528U